Advances in POST2 End-to-End Descent and Landing Simulation for the ALHAT Project

Jody L. Davis[*], Scott A. Striepe[†], Robert W. Maddock[‡] and Glenn D. Hines[§]
NASA Langley Research Center, Hampton, VA, 23681

Stephen Paschall II[**], Babak E. Cohanim[††], Thomas Fill[‡‡] and Michael C. Johnson[§§]
Charles Stark Draper Laboratory, Cambridge, MA, 02139

Robert H. Bishop[***] and Kyle J. DeMars[†††]
The University of Texas at Austin, Austin, TX, 78712

Ronald R. Sostaric[‡‡‡]
NASA Johnson Space Center, Houston, TX, 77058

and

Andrew E. Johnson[§§§]
Jet Propulsion Laboratory, Pasadena, CA, 91109

Program to Optimize Simulated Trajectories II (POST2) is used as a basis for an end-to-end descent and landing trajectory simulation that is essential in determining design and integration capability and system performance of the lunar descent and landing system and environment models for the Autonomous Landing and Hazard Avoidance Technology (ALHAT) project. The POST2 simulation provides a six degree-of-freedom capability necessary to test, design and operate a descent and landing system for successful lunar landing. This paper presents advances in the development and model-implementation of the POST2 simulation, as well as preliminary system performance analysis, used for the testing and evaluation of ALHAT project system models.

Nomenclature

$\vec{a}_{acc}$ = accelerometer measured acceleration vector
$\vec{a}_{env}$ = true (environment) body acceleration vector
$\vec{b}_{acc}$ = accelerometer bias
$\vec{b}_{gyro}$ = gyroscope bias

[*] Aerospace Engineer, Atmospheric Flight and Entry Systems Branch, MS 489, AIAA Member.
[†] Senior Aerospace Engineer, Atmospheric Flight and Entry Systems Branch, MS 489.
[‡] Senior Aerospace Engineer, Atmospheric Flight and Entry Systems Branch, MS 489, AIAA Senior Member.
[§] Senior Electronics Engineer, Flight Software Systems Branch, MS 472.
[**] Senior Member of the Technical Staff, GNC Systems—Mission Design, AIAA Member.
[††] Systems Engineer, Space Systems, 555 Technology Square/MS 27.
[‡‡] Principal Member Technical Staff, GN&C Systems Division, MS 70, AIAA Member.
[§§] Senior Member Technical Staff, Aerospace G&C, 555 Technology Square/ MS 70, AIAA Member.
[***] Professor, Aerospace Engineering & Engineering Mechanics, WRW215FA, AIAA Fellow.
[†††] Graduate Research Assistant, Aerospace Engineering & Engineering Mechanics,WRW411C, AIAA Member.
[‡‡‡] Aerospace Engineer, Flight Mechanics and Trajectory Design Branch, Mailcode EG5, AIAA Senior Member.
[§§§] Principal Member Technical Staff, Optical Navigation Group—GN&C Section, MS 301-121, AIAA Member.

$\vec{b}_{st}$ = star tracker bias
$\bar{q}_{e(b,\eta)}$ = attitude error quaternion
$\bar{q}_{env}$ = true (environment) attitude quaternion
$\bar{q}_{st}$ = star tracker measured attitude quaternion
SF_{acc} = accelerometer scale factor diagonal matrix
SF_{gyro} = gyroscope scale factor diagonal matrix
$\vec{\eta}_{acc}$ = accelerometer noise
$\vec{\eta}_{gyro}$ = gyroscope noise
$\vec{\eta}_{st}$ = star tracker noise
$\vec{\omega}_{env}$ = true (environment) body angular rate vector
$\vec{\omega}_{gyro}$ = gyroscope measured angular rate vector

I. Introduction

THE Autonomous Landing and Hazard Avoidance Technology (ALHAT) project[1] consists of a multi-center team composed of NASA centers, academia, and industry, with a common goal to develop an autonomous lunar precision-landing system for robotic and crew-piloted lunar descent vehicles. This system will have the capability to detect and avoid surface hazards for safe and repeated landings on the surface of the moon. Program to Optimize Simulated Trajectories II (POST2)[2] is used as a basis for an end-to-end, six-degree-of-freedom (6DOF) descent and landing trajectory simulation that is central to determining system performance of various lunar landing subsystem models and environment models (i.e. gravity and topography) for the ALHAT project. The lunar landing subsystem is comprised of Autonomy, Guidance, Navigation and Control (AGNC) and Hazard Detection and Avoidance (HDA) algorithms, as well as sensor models such as Inertial Measurement Unit (IMU), star tracker, altimeter, velocimeter, Terrain Relative Navigation (TRN) and light detection and ranging (LIDAR). POST2 provides descent and landing simulation capability to design a descent and landing system for successful lunar landing. It should be noted that the POST2 trajectory simulation and model implementations described in this paper are either updated from a previous ALHAT POST2 conference paper[3] or new to the simulation. Any ALHAT lunar landing subsystem model or environment model that has not been changed or updated in the POST2 simulation since Ref. 3 will not be presented here.

II. Trajectory Development and Simulation

The ALHAT end-to-end, descent and landing trajectory development has progressed with advancements in the descent and landing trajectory simulation in POST2 as well as updates of previous models or the inclusion of new models. This simulation uses six degrees-of-freedom (6DOF), integrating translational and rotational equations of motion along the trajectory. POST2 is a generalized point mass, discrete parameter targeting and optimization trajectory simulation program used for mission and system development support, engineering trade studies, development of reference trajectories, and mission planning and operation support at NASA Langley Research Center. POST2 has the ability to simulate three-degree-of-freedom (3DOF), 6DOF, and multi-degree-of-freedom trajectories for multiple vehicles, simultaneously, in various flight regimes. POST2 also has the capability to incorporate various gravity, vehicle, propulsion, guidance, control, sensor and navigation system models.

The POST2 descent and landing trajectory simulation supports ALHAT systems preliminary and detailed design, development, testing, and operations by establishing an end-to-end simulation that incorporates the latest engineering models of the ALHAT lunar descent and landing systems and the lunar environment. The ALHAT POST2-based descent and landing simulation has been updated to include models developed and validated to provide a 6DOF-capability. The POST2 software incorporates the ALHAT project-defined lunar lander vehicle model, propulsion model, lunar 165x165 degree spherical harmonic gravity-field model and 0.25 degree grid-spacing lunar topography model[3]. Low fidelity, statistically based sensor models such as IMU and accelerometer, star tracker, altimeter, velocimeter and TRN are also currently included in the POST2 software. Higher fidelity LIDAR sensor models made available through the ALHAT project are also incorporated. The addition of even higher-fidelity ALHAT-specific lunar-landing system models, as the models mature, will be incorporated into the simulation.

The current ALHAT POST2-based descent and landing nominal simulation begins with initialization of the vehicle truth state (i.e., position, velocity, attitude and attitude rate), as well as the navigated state. The ALHAT POST2 simulation is based on a series of trajectory events and criteria that define key phases of a representative ALHAT trajectory sequence. The current reference trajectory is derived from an optimal descent profile initiated from a circular lunar orbit. A de-orbit burn event, with a nominal ΔV of about 20 m/s from a 100 km orbit, is performed to reach a periapsis altitude of approximately 15 km. Altitude measurement updates begin at an altitude of approximately 20 km. The braking phase (which also includes the TRN portion of the trajectory) begins with powered descent ignition (PDI) to reduce velocity from orbital speeds at a nominal altitude of approximately 15 km. During the braking phase, a TRN sensor measurement event begins at an altitude of 15 km and terminates at 5 km. Sensor-model velocity measurement updates begin at an altitude of 2 km. These altitude, velocity and terrain-relative measurements are used by the navigation filter to update the estimated state (inertial position and velocity) of the landing vehicle during descent. The approach phase of the trajectory, which is triggered at a nominal altitude of approximately 1 km, begins with vehicle pitch-up and throttle-down, targeting a point in space directly above the landing site. During this phase, the Hazard Detection and Avoidance (HDA) and Hazard Relative Navigation (HRN) portion of the trajectory also begin. The vehicle remains in the approach phase until the start of vertical descent to the targeted landing site, with constant rate of descent beginning at approximately 30 m above the lunar surface. Figure 1 shows an example of a representative ALHAT POST2-based descent and landing sequence of events and timeline.

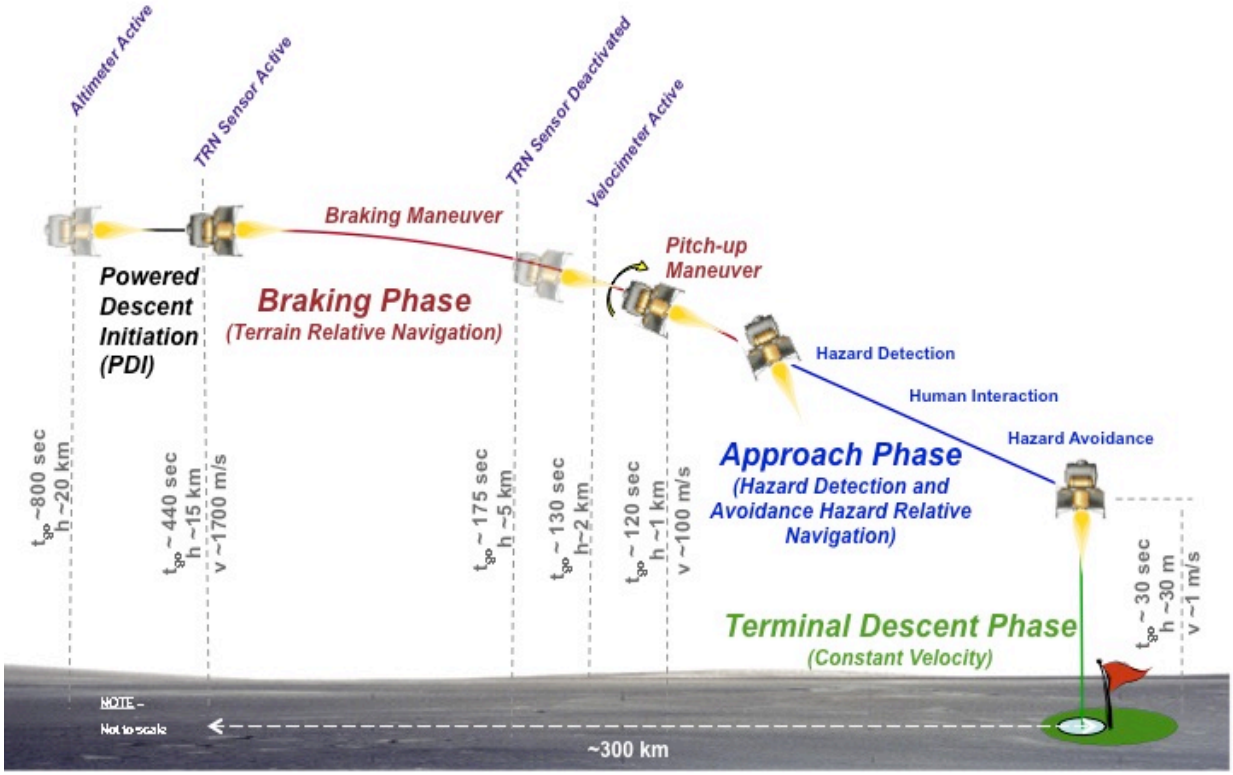

Figure 1. Example of ALHAT POST2 trajectory sequence and timeline.

III. Simulation Model Implementation

The following sections describe in detail updated and new ALHAT subsystem models incorporated into the current end-to-end, ALHAT POST2-based trajectory simulation. These models are integrated into the simulation and have been tested and validated. A flight software module (FSW) is incorporated into the ALHAT POST2-based simulation to act as an interface between each ALHAT-specific model, lunar environment models, vehicle model and the main (core) POST2 program that contains the dynamics and integration of the simulation as well as I/O and data handling. FSW in POST2 allows for independent control of the data and update rates required from each model and provides control over the flow of information. Figure 2 shows a flow chart of the interaction of POST2, FSW and lunar- and ALHAT-specific models. The lunar environment encompasses the lunar gravity, topography, and

terrain models. The ALHAT-specific sensor models include TRN, HRN, and flash and scanning LIDAR models. The LIDAR models are coupled with Hazard Detection and Avoidance (HDA) algorithms and packaged into a Terrain Sensing and Recognition (TSAR) model. TSAR will be discussed in more detail in the following sections. The sensor models labeled as "OTHER SENSORS" in Fig. 2 that are not detailed in the diagram include the IMU, star tracker, altimeter and velocimeter models in the POST2-based simulation. It is noted that as the ALHAT project matures and higher fidelity ALHAT-specific models, such as TRN, HRN, and altimeter and velocimeter models become available, they will be integrated and validated in the ALHAT POST2-based simulation.

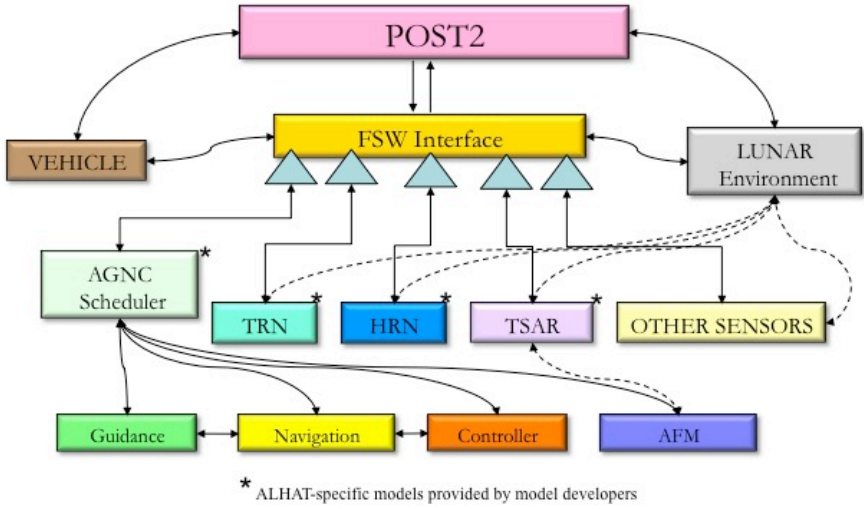

Figure 2. POST2-FSW and ALHAT-specific software interaction flow chart

A. Vehicle Model

The ALHAT project-defined, Exploration Systems Architecture Study (ESAS)-derived, vehicle model shown in Fig. 3 is used in the ALHAT POST2-based simulation for the first phases of the ALHAT system performance analysis or Design Analysis Cycle (DAC). This model is an Apollo-like, four-legged landing gear configured lunar-lander containing a single pump-fed, oxygen-hydrogen propulsion, two-axis gimbaled descent engine. This main engine is located on the vehicle centerline, and has a maximum thrust capability of 357,081 N, specific impulse of 440 seconds, and is throttleable from 10% to 100%. The vehicle also has 16 Reaction Control System (RCS) thrusters that each have a 445 N thrust capability and specific impulse of 225 seconds, and are located 2.6 m from the top of the vehicle. The total height of the vehicle is 10.5 m with a base maximum leg span of 12.0 m. The total mass input into the POST2-based simulation at low lunar orbit (before the de-orbit burn is performed) is 42,284 kg, which corresponds to a landed mass of approximately 27,155 kg. Figure 3 also shows the geometry of the ALHAT-defined vehicle and the center of gravity (CG) with respect to the POST2-defined body reference frame, the ALHAT-defined structural frame, and the POST2-defined body-centered frame. The POST2 body reference axes (x_{BR}, y_{BR}, and z_{BR}) are aligned

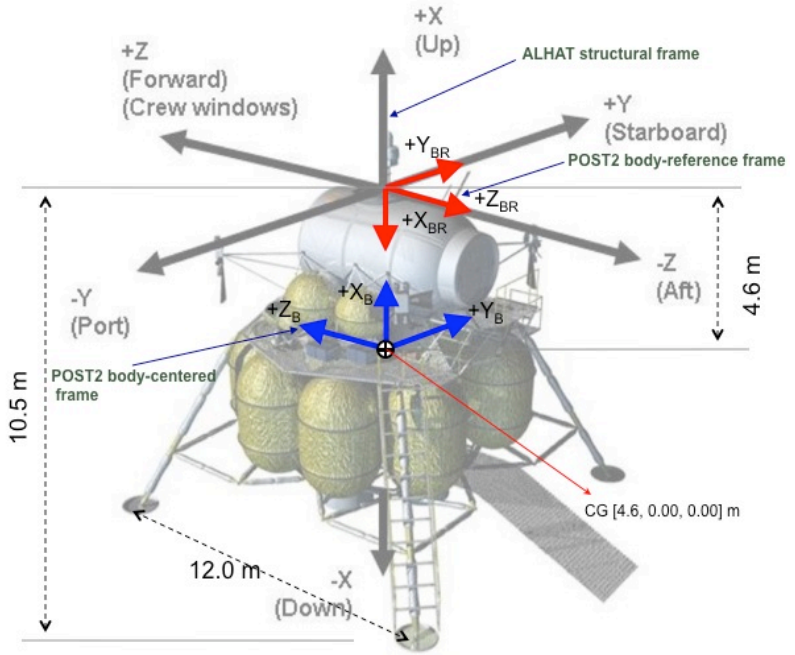

Figure 3. ALHAT-defined vehicle model in POST2 simulation.

as shown with its origin at the docking interface at the top of the vehicle, x-axis pointing toward the base of the lander, z-axis pointing aft of the crew windows, and the y-axis completing the right hand system. The POST2 body-centered axes (x_B, y_B, and z_B) are aligned as shown with its origin at the CG (moving with the CG), x-axis pointing toward the top of the vehicle along the centerline, z-axis pointing toward the crew windows, and the y-axis completing the right hand system. The ALHAT-defined structural axes are aligned as shown with its origin at the docking interface, x-axis pointing up from the base of the lander, z-axis pointing forward toward the crew windows, and the y-axis completing the right hand system; note that the ALHAT-defined structural axes and POST2 body-centered axes are parallel. Input CG, inertias, and engine locations from the ALHAT-specific models, with respect to the ALHAT-defined structural frame, are transformed to the POST2 body reference frame for input into the POST2 simulation.

B. Low-Fidelity Sensor Models

1. Low-Fidelity IMU Model

The POST2-developed IMU model in the ALHAT POST2 software is a low-fidelity, statistically based accelerometer and gyroscope model. The accelerometer model takes the true (environment) body acceleration, along with a random bias, noise, and scale factor errors to generate a measurement of accelerations that are then passed to Navigation for processing. The acceleration measurement model is given by:

$$\vec{a}_{acc} = \left(I_{3\times 3} + SF_{acc}\right)\vec{a}_{env} + b_{acc} + \eta_{acc}, \tag{1}$$

where

$$SF_{acc} = \begin{bmatrix} SF_{acc(x)} & 0 & 0 \\ 0 & SF_{acc(y)} & 0 \\ 0 & 0 & SF_{acc(z)} \end{bmatrix}, \quad \vec{b}_{acc} = \begin{bmatrix} b_{acc(x)} \\ b_{acc(y)} \\ b_{acc(z)} \end{bmatrix}, \quad \vec{\eta}_{acc} = \begin{bmatrix} \eta_{acc(x)} \\ \eta_{acc(y)} \\ \eta_{acc(z)} \end{bmatrix} \tag{2}$$

and $\vec{a}_{acc}$ is the accelerometer measured acceleration vector in m/s^2, $\vec{a}_{env}$ is the true (environment) body acceleration vector in m/s^2, I_{3x3} is the identity matrix, SF_{acc} is the accelerometer scale factor diagonal matrix, $\vec{b}_{acc}$ is the accelerometer bias and $\vec{\eta}_{acc}$ is the random noise. The accelerometer measurement updates begin at the start of the trajectory, and continue until touchdown at a rate of 200 Hz. The gyroscope model takes the true (environment) body angular rates, with a random noise, bias and scale factor errors to generate a measurement of angular rates that are passed to Navigation. Similar to the accelerometer Eq. (1) and Eq. (2), the gyroscope angular rate measurement model is given by:

$$\vec{\omega}_{gyro} = \left(I_{3\times 3} + SF_{gyro}\right)\vec{\omega}_{env} + \vec{b}_{gyro} + \vec{\eta}_{gyro}, \tag{3}$$

where $\vec{\omega}_{gyro}$ is the gyroscope measured angular rate vector in rad/s, $\vec{\omega}_{env}$ is the true (environment) body angular rate vector in rad/s, SF_{gyro} is the gyroscope scale factor diagonal matrix, b_{gyro} is the gyroscope bias and η_{gyro} is the random noise. The gyroscope measurement updates also begin at the start of the trajectory and continue until touchdown at a rate of 200 Hz.

2. Low-Fidelity Star Tracker Model

The POST2-developed star tracker model in the ALHAT POST2 simulation is a low-fidelity, statistically based model. The star tracker model takes the true attitude quaternion, bias and noise to generate a star tracker measurement that is then passed to Navigation for processing as an external measurement. The noise ($\vec{\eta}_{st}$) and bias ($\vec{b}_{st}$) are used as such to calculate an error quaternion ($\overline{q}_{e(b,\eta)}$) via

$$\bar{q}_{e(b,\eta)} = \begin{bmatrix} \cos\left(\frac{\beta_{st}}{2}\right) \\ \frac{\vec{\beta}_{st}}{\beta_{st}} \sin\left(\frac{\beta_{st}}{2}\right) \end{bmatrix}, \tag{4}$$

where

$$\begin{aligned} \vec{\beta}_{st} &= \vec{\eta}_{st} + \vec{b}_{st}, \\ \beta_{st} &= \left\| \vec{\beta}_{st} \right\| \end{aligned} \tag{5}$$

The star tracker measured attitude quaternion ($\bar{q}_{st}$) is found as the product of the true quaternion ($\bar{q}_{env}$) and error quaternion ($\bar{q}_{e(b,\eta)}$) yielding

$$\bar{q}_{st} = \bar{q}_{e(b,\eta)} \bar{q}_{env} \tag{6}$$

The star tracker measurement updates begin at the start of the trajectory and continue until touchdown at a rate of 1 Hz.

3. Low-Fidelity Terrain Relative Navigation and Hazard Relative Navigation Model

Terrain Relative Navigation (TRN) and Hazard Relative Navigation (HRN) are terrain-mapping capabilities used for accomplishing safe, precision landing on the surface of the moon by providing the navigation filter with three-dimensional position measurements. These terrain-mapping capabilities are facilitated by terrain sensor data-processing with terrain-mapping algorithms.[9] The ALHAT-specific TRN model is currently a low-fidelity model implemented into the ALHAT POST2-based simulation. During the TRN phase of the descent trajectory shown previously in Fig. 1, the TRN sensor model is active from 15 km altitude down to 5 km altitude and measurements are taken at a rate of 0.5 Hz. Specifically for the ALHAT POST2-based simulation, the low-fidelity TRN model determines the landing vehicle three-dimensional position, with random noise applied (as a function of altitude) for dispersion analysis, in a pre-defined ALHAT-specific lunar-surface lunar-fixed (LSLF) coordinate system with its origin at the landing site location. The TRN sensor measured surface-fixed position is then passed to the Navigation system for processing. It is noted that this low-fidelity TRN model in POST2 does not currently account for map-tie errors, but will be updated with increasing fidelity as the ALHAT system matures. Also, a low-fidelity HRN model is currently not available in the POST2 software but is in the development stages. Therefore, the performance analysis of the ALHAT system and POST2 simulation in this paper does not currently include HRN measurements.

C. Autonomy Guidance Navigation and Control Model

The ALHAT Autonomy, Guidance, Navigation and Control (AGNC) software system integrated into the POST2-based simulation provides state estimation and closed-loop control of the landing vehicle to enable safe and precise lunar landing. As currently configured, the system is initialized in lunar orbit with a moderate quality state estimate and covariance, such as would be provided by external earth-based tracking. From this point the system will, if given authority to proceed, commence the automated landing process. In addition to the automated landing capability, the system will determine (or accept in the case of human interaction) and divert to landing target redesignations at any point along the trajectory, until the point when the vehicle control authority is no longer sufficient to perform this maneuver. These divert maneuvers are intended primarily as hazard avoidance maneuvers, with the assumption that either human eyes or an onboard sensor system can observe the terrain at the landing site and recommend a safe point to land. Thus, this AGNC system will be extended to support robotic and human-in-the-loop spacecraft control in the event that the landing vehicle is teleoperated or flown by crew on board. The goal of this AGNC system design is to work in conjunction with terrain navigation and hazard detection sensors to enable "anytime, anywhere" safe precision lunar landings.

The ALHAT Navigation algorithm is a dual-state extended Kalman filter (EKF). The responsibility of ALHAT Navigation is to provide estimates of the spacecraft state (position, velocity, and attitude) and landing site location (addressing map tie errors) to other subsystems at required rates in required frames. Navigation processes

external sensor measurements aided by a strap-down IMU and utilizes a dual-state strategy including the inertial state of the spacecraft, the location of the landing target site, various sensor error and un-modeled acceleration estimates. Navigation also provides a user parameter processing capability (UPP) that computes estimates of requested parameters (e.g., spacecraft position) at higher rates than navigation is executing. The navigation filter design is a recursive nonlinear filter capable of asynchronous fusion of measurements from various sensors including an altimeter, velocimeter, star tracker, and TRN sensor. The EKF combines the inertial data from the IMU with star tracker attitude measurements early in the landing mission to estimate the vehicle state. At about a 20 km altitude, an altimeter begins providing measurements to Navigation that significantly improves both the altitude and downrange position estimates. Additional measurements are obtained by a TRN sensor that enables Navigation to correct for map-tie errors and further improve the state estimate. Once the vehicle is within a 2 km altitude, Navigation will begin processing velocimeter measurements to further improve the state estimate prior to landing. If a hazard detection sensor is on board, information of the vehicle's location relative to the local hazards can be used as an additional source of terrain-relative measurements. In the current form, the EKF captures the Apollo and Space Shuttle heritage. To date, the design strategy has been to include as much model complexity as possible in the initial "optimal" design. Then the complexity will be systematically reduced while at each stage attempting to retain as close to the optimal performance as possible with tuning[4,5,6].

The ALHAT Guidance algorithm provides a burn targeting function to initiate the powered maneuvers, determining the nominal burn ignition and cutoff times to achieve a landing at the specified target. During execution of the descent trajectory, this targeting mechanism also corrects the ignition and cutoff times as needed to compensate for trajectory dispersions due to maneuver execution error, environment uncertainty, and Navigation updates. During each powered maneuver the algorithm provides burn guidance, or the burn direction and magnitude information needed to complete the maneuvers. For the deorbit and braking maneuvers, Guidance utilizes an evolution of the Space Shuttle Powered Explicit Guidance (PEG) algorithm. The braking algorithm provides full state vector control to ensure the vehicle arrives at the desired target relative initial conditions of the approach phase. For the terminal maneuvers, Guidance utilizes explicit analytic solutions to polynomials in time. The polynomial selections are based on fuel efficiency and constraints, and provide hazard avoidance maneuver capability with a terminal attitude constraint for touchdown.

The ALHAT control algorithm[7] takes the Guidance commands as input and manages the vehicle RCS system, the main engine throttle, and the main engine gimbal to enable the maneuvers and landing. Pitch and yaw control during the burn is enabled through Thrust Vector Control (TVC) of the main engines using a Proportional-Integral-Derivative (PID) controller. The RCS control is accomplished by a Phase Plane design for all attitude channels during coast and for roll during a burn.

The ALHAT Autonomous Flight Manager (AFM)[8] is the autonomous capability for the AGNC subsystem, providing the following functionality throughout the mission: authority to proceed to the next mission phase, trajectory management, and sensor management. Prior to the deorbit maneuver and PDI, the AFM either determines whether it is safe to proceed (robotic missions), or prompts the crew for a decision (human missions). During the descent, the AFM determines the need to re-designate the landing point, evaluates unacceptable variance from the nominal state for the vehicle throughout the trajectory, and sets up sensor pointing for the TRN and HDA functions. It is noted that AFM performance in the ALHAT POST2 simulation is not presented in this paper, but AFM functionality required for the HDA phase of the mission is being analyzed in the first ALHAT Design Analysis Cycle (DAC1).

D. Terrain Sensing and Recognition and Hazard Detection and Avoidance

Terrain Sensing and Recognition (TSAR) is ALHAT-specific software integrated into the POST2-based simulation that currently incorporates LIDAR sensor models and a Hazard Detection and Avoidance (HDA) algorithm. Each LIDAR model uses POST2-generated true (environment) trajectory data and a truth digital terrain map to produce simulated sensor-acquired image data that is then corrected based on the navigated (estimated) spacecraft motion. The simulated images are currently collected as a mosaic of scans over an area of the lunar surface surrounding the landing site. Both scanning and flash LIDAR models are integrated into the POST2 simulation so that trade studies may be performed. Both sensors also use a LASER as an illumination source. In the case of scanning LIDAR, the LASER is scanned across the scene and the data is collected by a single detector as a series of points. Since only one point is illuminated and detected these systems often have good range operation, however all points collected during a scan must then be re-aligned compensating for spacecraft motion to create an

image. For flash LIDAR, the LASER illuminates the scene and a 2-dimensional focal plane array collects all points within a scan area simultaneously. Range and intensity image are generated at up to 30 images per second. Once the mosaic is complete, the simulated sensor output image is then passed to the HDA algorithm to generate a lunar hazard map.

The ALHAT project HDA[9] approach is based on imaging LIDAR and an efficient HDA algorithm. The HDA algorithm first transforms a mosaic of LIDAR images (represented as clouds of 3D points) from the sensor frame to local level frame using on-board navigation state information. A digital elevation map (DEM) is then constructed from the transformed points and local operators are applied to the DEM to detect regions of high slope and roughness. Slope and roughness is threshold to establish a binary terrain hazard map. A distance transform is applied to the hazard map to create a Distance to Nearest Hazard (DTNH) map that is then passed on to AFM for safe site selection. The DTNH map gives distance to the nearest hazard from the edge of the Vehicle Footprint Dispersion Ellipse (VFDE).

The purpose of HDA, as incorporated in the ALHAT POST2 simulation, is to autonomously detect lunar surface hazards near the landing site. Landing hazards exist everywhere on the lunar surface and many desirable landing sites are near the most hazardous terrain (e.g., the rim of Shackleton Crater), so HDA is critical to autonomously and safely land payloads over much of the lunar surface. The HDA requirements used in the ALHAT project are to detect hazards that are 0.3 m tall or higher and slopes that are 5 degrees or greater. It should be noted that TSAR performance in the ALHAT POST2 simulation is not presented in this paper but is currently being analyzed for the TSAR portion of DAC1.

IV. Design Analysis Cycle Results

The first ALHAT Design Analysis Cycle (DAC1) includes Monte Carlo trajectory analyses that focus on the ALHAT GNC and TSAR systems. The main focus of this paper is the GNC system portion of the Monte Carlo trajectories. A set of eight ALHAT POST2 Monte Carlos were run to analyze the statistics of the preliminary performance of the closed-loop GNC and to assess the Vehicle Footprint Dispersion Ellipse (VFDE) size. The set of GNC Monte Carlos analyzed in this paper were performed with Navigation active, sending Guidance and the Controller the navigated (estimated) state, while perturbing not only vehicle properties such as engine thrust, specific impulse and mass properties, but sensor errors and the navigated initial state, to address the Navigation performance. The Monte Carlos consist of eight sets (Apollo, Brakes, Cheapo, Nominal, Peeky, Sensor, Slanty and Stretch) of 2000 dispersed trajectories each, each representing a different approach phase design which are taken from the larger ALHAT trade space for DAC1. In the following sections, the Monte Carlo inputs used for DAC1 and a preliminary analysis of the DAC1 GNC Monte Carlo results are discussed. The requirements being addressed for this first set of results of DAC1 are landing accuracy of a 1-sigma downrange and crossrange variation of less than 30 m. Preliminary touchdown requirements used to assess the integrated system performance consist of a 99-percentile vertical velocity less than 2 m/s, 99-percentile horizontal velocity less than 1 m/s and 99-percentile attitude rate (RSS of pitch and yaw rate) less than 2 deg/s. Another preliminary touchdown requirement is that the vehicle must be close to vertical; that is, that the 1-percentile relative pitch angle of the lander must be greater than 84 deg.

A. GNC Monte Carlo Inputs

A portion of the input parameters varied for the DAC1 GNC Monte Carlos consist of vehicle dispersions, namely main engine thrust and specific impulse, RCS jet thrust and specific impulse, vehicle CG location and moments of inertia. Table 1 shows the dispersed Monte Carlo parameters, dispersions and dispersion type for perturbed vehicle properties in DAC1.

Table 1. GNC Monte Carlo vehicle input dispersions for DAC1.

Parameter			*Dispersion*		
		Mean	**Max/Min**	**Units**	**Type**
Main Engine	Thrust	89,271	+/- 890	N	Uniform
	I_{sp}	440	+/- 2	sec	Uniform
RCS	Thrust	445	+/- 22 (3-sigma)	N	Gaussian
(for each jet)	I_{sp}	225	+/- 10	sec	Uniform
Gimbal	no engine gimbal dispersion				
Mass properties	X cg location	-	+/- 0.21	m	Uniform
	Y cg location	-	+/- 0.10	m	Uniform
	Z cg location	-	+/- 0.10	m	Uniform
	Mass	42,284	+/- 1269	kg	Uniform
	Ixx	1	+/- 10%	%	Uniform
	Iyy	1	+/- 10%	%	Uniform
	Izz	1	+/- 10%	%	Uniform
	Ixy	0	+/- 330	$kg\text{-}m^2$	Uniform
	Ixz	0	+/- 330	$kg\text{-}m^2$	Uniform
	Iyz	0	+/- 18,200	$kg\text{-}m^2$	Uniform

In addition to vehicle parameters, sensor errors and the initial knowledge state are also varied for the DAC1 GNC Monte Carlos. Table 2 shows the dispersed Monte Carlo parameters, dispersions and dispersion type for perturbed sensors and initial knowledge state in DAC1.

Table 2. GNC Monte Carlo sensor and knowledge state input dispersions for DAC1.

Parameter			*Dispersion*		
		Mean	**3-sigma**	**Units**	**Type**
Sensors					
Accelerometer	bias	0	+/- 0.0009	m/s^2	Gaussian
(same error for each direction)	scale factor	0	+/- 1.98e-04	%	Gaussian
	random noise		+/- 0	m/s^2	Gaussian
Gyro	bias	0	+/- 2.91e-07	rad/s	Gaussian
(same error for each direction)	scale factor	0	+/- 4.8e-06	%	Gaussian
	random noise		+/- 0	rad/s	Gaussian
Startracker	bias	0	+/- 0.1668	deg	Gaussian
(same error for each direction)	random noise		+/- 0.417	deg	Gaussian
Altimeter	bias	0	+/- 0.3	m	Gaussian
	scale factor	0	+/- 0.3	%	Gaussian
	random noise		• +/- 60 (20 km altitude) • +/- 19.8 (2 km altitude)	m	Gaussian
Velocimeter	bias	0	+/- 0.03	m/s	Gaussian
	scale factor	0	+/- 0.3	%	Gaussian
	random noise		+/- 0.09	m/s	Gaussian
TRN	random noise		• +/- 24.7 (12–15km altitude) • +/- 0.3% altitude – 14.0 (7–12 km altitude) • +/- 8.6 (5–7 km altitude)	m	Gaussian
Initial States					
NAV States	inertial position (xi, yi, zi)		+/- 4340 (xi) +/- 600 (yi) +/- 1212 (zi) (position error from NAV covariance)	m	Gaussian
(2000 dispersed NAV states in file)	inertial velocity (vxi, vyi, vzi)		+/- 1.21 (vxi) +/- 0.60 (vyi) +/- 4.34 (vzi) (velocity error from NAV covariance)	m/s	Gaussian

B. GNC Monte Carlo Results Summary

Several key output parameters for each of the eight different approach phase designs (Apollo, Brakes, Cheapo, Nominal, Peeky, Sensor, Slanty and Stretch) were investigated to assess system performance. These key output parameters consist of downrange and crossrange, timeline from approach start to the constant velocity subphase of the terminal descent phase (time available for the HDA portion of the trajectory), altitude margin from approach start to the constant velocity subphase (altitude available for the HDA portion of the trajectory), horizontal and vertical surface-relative velocity at touchdown, vehicle attitude and attitude rate at touchdown.

Starting with the approach phase of the trajectory (highlighted in Fig. 4), the lunar lander has performed the vehicle pitch-up maneuver and throttle-down, targeting a point in space directly above the landing site. In Table 3, the eight approach phase designs are characterized by the slant range and slant angle with respect to the landing site target at the start of approach. For example, the Sensor approach phase design has a mean slant range of 1030 m and a mean slant angle of 88 deg, the largest angle of the eight cases, thus providing a more optimal perspective for LIDAR sensor measurements of the lunar surface. The values shown in Table 3 also serve to verify that the trajectory simulations capture the desired approach conditions for each of the eight cases guidance was targeting. Note that the maximum, minimum, 99-percentile and 1-percentile values given in the results are absolute and not relative to the mean.

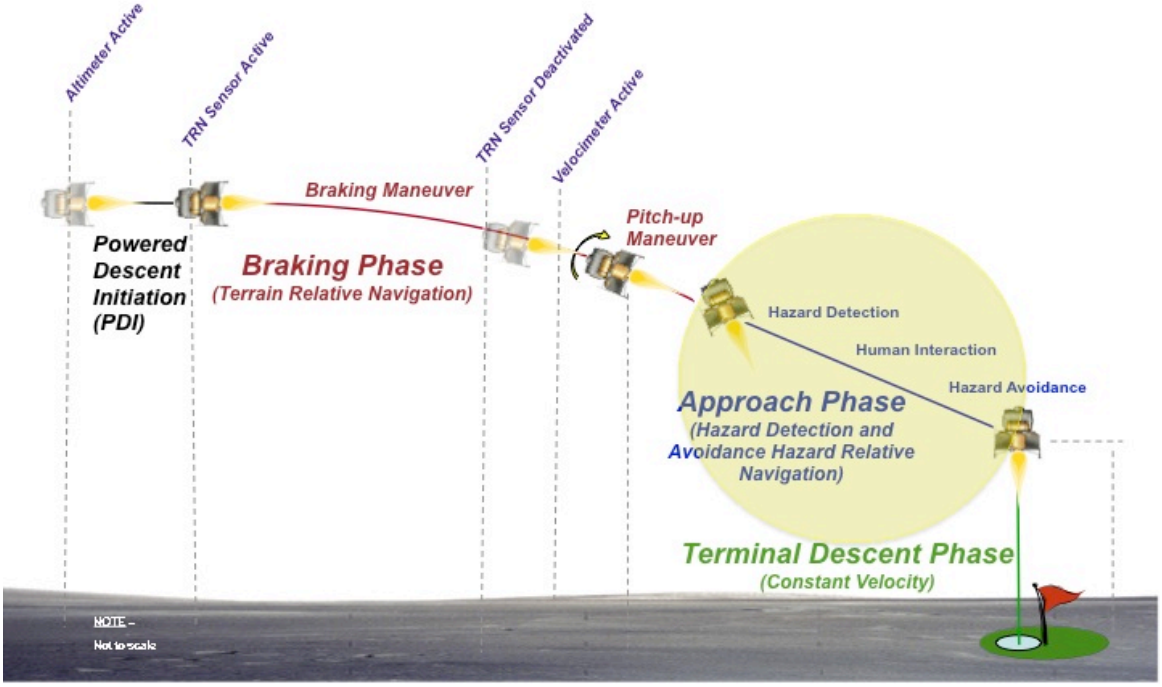

Figure 4. Approach phase of the ALHAT trajectory sequence.

The slant range and angle quantities in Table 3 confirm that the closed-loop Guidance/Control system is working in the presence of system uncertainties and navigation error. The approach phase includes the HDA and HRN portion of the trajectory where lunar-surface hazard maps are generated by the TSAR subsystem and then analyzed by AFM before commanding a divert maneuver to avoid surface hazards, if necessary. (Recall that the GNC Monte Carlos analyzed and presented in this paper do not include TSAR, AFM and divert performance, or in other words, the HDA and HRN portion of the trajectory is not simulated in this analysis of GNC Monte Carlos.) The timeline and altitude from the start of the approach phase to the constant velocity subphase at this point in the trajectory are essential for giving ample margin to perform such tasks. In Table 3, it is shown that the Cheapo (lowest propellant consumption case) and Slanty case have the smallest timeline (1-percentile) of 40 sec, which is a significant difference between the largest timeline (1-percentile) of 93 sec from the Stretch case. The Stretch case also has the largest altitude margin (1-percentile) of 1393 m, which gives generous timeline and altitude margin to analyze hazard maps and perform a divert if required. The Slanty case also has the smallest altitude margin (1-

percentile) of only 211 m, in addition to the smallest timeline. These timeline margins will be further evaluated during the TSAR portion of DAC1 analyses.

Table 3. Key POST2 GNC Monte Carlo parameters (Approach).

Requirement / Design Constraint	*Value*	*Units*	*Apollo*	*Brakes*	*Cheapo*	*Nominal*	*Peaky*	*Sensor*	*Slanty*	*Stretch*
Start of Approach Phase										
Slant Range to Target	**Mean**	**m**	**2044.4**	**511.5**	**839.5**	**1029.0**	**1026.3**	**1028.1**	**524.2**	**2042.2**
	1-sigma	m	43.3	29.8	27.6	27.2	20.8	11.5	38.7	29.4
	Max	m	2205.4	623.7	942.3	1127.5	1092.1	1061.1	647.2	2135.8
	Min	m	1897.5	398.1	754.2	919.2	965.5	1001.2	397.1	1936.3
	99%-tile	m	2147.7	582.4	900.4	1088.9	1073.4	1051.0	619.3	2109.8
	1%-tile	m	1942.1	443.9	781.4	968.1	979.6	1005.7	434.1	1974.3
Slant Angle to Target	**Mean**	**deg**	**14.9**	**45.1**	**44.8**	**44.9**	**59.9**	**88.2**	**29.9**	**44.9**
	1-sigma	deg	0.4	3.3	1.9	1.5	1.8	1.1	2.7	0.8
	Max	deg	16.2	61.0	51.1	51.1	66.5	90.0	42.6	47.6
	Min	deg	13.7	35.2	39.8	40.7	54.2	82.5	22.2	42.8
	99%-tile	deg	15.9	52.8	49.2	48.4	64.0	89.8	36.8	46.7
	1%-tile	deg	14.0	37.2	40.7	41.6	56.0	85.0	24.3	43.2
During Approach Phase										
Total Time from Approach to Constant Velocity SubPhase *(Available time for HDA and divert)*	Mean	sec	99.2	82.8	39.7	66.6	71.1	61.6	41.6	95.9
	1-sigma	sec	4.0	3.7	0.4	1.1	1.1	0.7	1.0	1.5
	Max	sec	111.0	94.2	41.2	70.4	74.2	63.4	46.6	102.2
	Min	sec	89.4	74.6	38.4	63.6	68.0	59.6	37.0	92.0
	99%-tile	sec	107.8	91.0	40.6	68.8	73.6	63.0	43.8	99.0
	1%-tile	**sec**	**91.8**	**76.0**	**38.8**	**64.2**	**69.0**	**60.2**	**38.6**	**93.0**
Selenodetic Altitude Margin from Approach to Constant Velocity SubPhase *(Available altitude margin for HDA and divert)*	Mean	m	496.9	329.5	559.9	694.6	856.4	996.2	228.9	1410.2
	1-sigma	m	9.8	9.2	10.1	9.6	9.4	9.2	9.6	9.5
	Max	m	518.5	347.6	580.3	714.0	874.3	1014.8	249.2	1429.7
	Min	m	475.2	309.5	536.4	672.3	834.5	976.8	206.9	1390.8
	99%-tile	m	514.3	345.9	578.5	712.8	873.9	1013.1	246.1	1428.7
	1%-tile	**m**	**478.2**	**312.5**	**541.2**	**677.3**	**839.2**	**979.2**	**210.7**	**1393.1**

Some of the requirements on the ALHAT lunar-landing system performance in the POST2-based simulation for DAC1 are currently at the touchdown event. One of the requirements is landing accuracy, defined by a 1-sigma downrange and crossrange variation of less than 30 m. The navigated range to target denotes the closed-loop Guidance/Control system performance. The Guidance system receives the vehicle state from the Navigation system only, which is based on the onboard knowledge state. Preliminary touchdown requirements used to assess the integrated system performance include a 99-percentile vertical velocity less than 2 m/s, 99-percentile horizontal velocity less than 1 m/s and 99-percentile attitude rate (RSS of pitch and yaw rate) less than 2 deg/s. The last touchdown preliminary requirement is that the vehicle must be close to vertical; that is, that the 1-percentile relative pitch angle of the lander must be greater than 84 deg. These preliminary touchdown requirements are Apollo-like or based on the Apollo program requirements[10]. Figure 5 shows the touchdown footprint, in terms of the ALHAT-defined LSLF coordinate frame, for each of the eight approach phase designs. Each data point represents one

dispersed case from its particular GNC POST2 Monte Carlo. There is minimal variation in the footprint size or placement between each of the eight cases. Table 4 contains key parameter data from the ALHAT POST2 GNC Monte Carlos at touchdown. Figure 5 illustrates the crossrange and downrange at touchdown data provided in Table 4. The 1-sigma variation of downrange to the target at touchdown is very similar (~30 to 32 m) for all eight Monte Carlos. Similarly, the 1-sigma variation of crossrange at touchdown is also similar (~7 to 10 m) for all eight Monte Carlos. Hence, regardless of which approach phase design is used, the landing accuracy requirement (highlighted in yellow) of a 1-sigma downrange and crossrange variation of less than 30 m is met for crossrange and extremely close (within a maximum of 7%) for downrange for this ALHAT DAC1. In addition, although there is no current requirement for total navigated range to target at touchdown, the total navigated range to target in Table 4 shows the performance of the ALHAT Guidance/Control system considering the 99-percentile value on average for all eight cases was only 4.5 m. This indicates excellent overall closed-loop Guidance/Control performance. The vertical and horizontal velocity at touchdown (99-percentile) for all eight approach phase designs met the preliminary requirement of less than 2 m/s and 1m/s, respectively, with little variation between cases. The preliminary requirement of attitude rate (RSS of pitch and yaw rate) at touchdown of less than 2 deg/s (99-percentile) was met for seven of the eight cases with little variation between cases; the highest attitude rate was 2.1 deg/s (99-percentile) for the Cheapo approach phase. Lastly, the vehicle orientation preliminary requirement at touchdown of 1-percentile relative pitch angle greater than 84 deg was also met for each approach phase design with no significant variation. Overall, for DAC1, the ALHAT GNC subsystem integrated into the POST2 simulation performed very well given the vehicle, navigation and sensor error uncertainties shown in Table 1 and Table 2. All of the current ALHAT preliminary requirements at touchdown were either met for all cases, or were within at least 7% of the requirement, with little to no variation between the different approach phase designs.

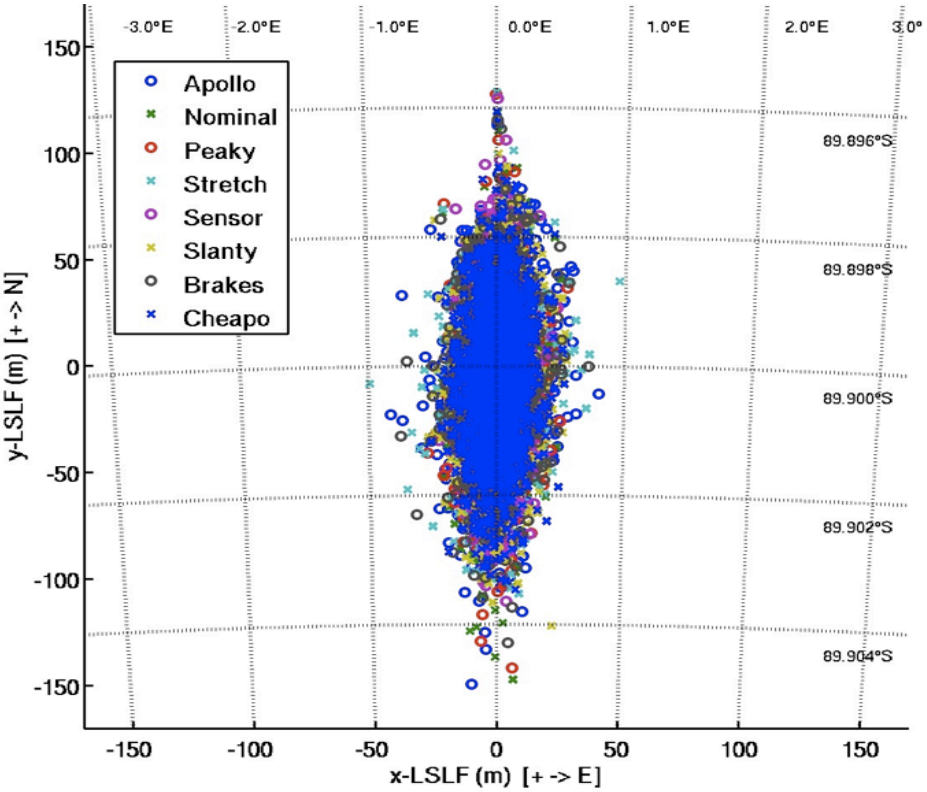

Figure 5. POST2 touchdown footprint of each approach phase design.

Table 4. Key POST2 GNC Monte Carlo parameters (Touchdown).

Requirement / Design Constraint	*Value*	*Units*	*Apollo*	*Brakes*	*Cheapo*	*Nominal*	*Peaky*	*Sensor*	*Slanty*	*Stretch*
Touchdown										
Crossrange	Mean	m	0.2	0.2	0.2	0.2	0.2	0.2	0.2	0.1
	1-sigma	**m**	**9.6**	**8.2**	**7.7**	**7.7**	**7.3**	**6.2**	**8.3**	**8.4**
	Max	m	42.2	38.0	28.1	27.1	29.5	25.3	29.0	51.0
	Min	m	-43.7	-39.4	-26.8	-28.3	-28.5	-23.7	-28.1	-52.4
	99%-tile	m	24.5	21.2	18.6	19.5	19.0	16.0	20.5	20.5
	1%-tile	m	-22.6	-19.4	-17.8	-17.8	-17.1	-14.9	-19.5	-21.8
Downrange	Mean	m	-6.4	-6.1	-6.4	-6.4	-6.5	-6.4	-6.3	-6.7
	1-sigma	**m**	**32.2**	**30.3**	**30.2**	**30.9**	**30.6**	**30.2**	**30.8**	**30.7**
	Max	m	114.0	115.4	119.7	119.0	127.7	125.6	100.0	128.7
	Min	m	-149.3	-129.9	-104.9	-147.2	-141.6	-110.3	-121.9	-106.8
	99%-tile	m	70.3	67.2	62.0	64.3	64.2	69.0	66.5	66.3
	1%-tile	m	-89.0	-79.5	-81.5	-86.3	-82.0	-78.7	-84.0	-85.0
Total Range to Target	Max	m	149.7	130.0	119.7	147.4	141.7	125.6	124.0	128.7
	Min	m	0.7	0.2	0.4	0.2	0.3	0.6	0.7	0.5
	99%-tile	m	90.3	81.4	85.0	89.0	83.8	81.2	85.4	85.6
	1%-tile	m	2.3	2.1	2.4	2.2	1.9	1.8	2.3	2.3
Total NAV Range to Target	Max	m	6.6	10.5	6.3	5.6	9.3	8.1	10.0	16.4
	Min	m	0.2	0.2	0.2	0.2	0.3	0.4	0.2	0.4
	99%-tile	m	3.8	4.0	4.6	4.3	4.7	5.6	4.0	5.3
	1%-tile	m	0.6	0.6	0.5	0.6	0.6	0.7	0.5	0.7
Vertical Velocity	Max	m/s	1.3	1.3	1.3	1.3	1.3	1.3	1.3	1.9
	Min	m/s	0.6	0.7	0.6	0.7	0.7	0.7	0.7	0.7
	99%-tile	**m/s**	**1.3**	**1.3**	**1.3**	**1.2**	**1.2**	**1.3**	**1.2**	**1.2**
	1%-tile	m/s	0.8	0.8	0.7	0.8	0.8	0.7	0.8	0.8
Horizontal Velocity	Max	m/s	1.0	5.9	0.4	1.0	1.4	1.2	2.5	4.9
	Min	m/s	0.0	0.0	0.0	0.0	0.0	0.0	0.0	0.0
	99%-tile	**m/s**	**0.3**	**0.5**	**0.3**	**0.2**	**0.3**	**0.3**	**0.3**	**0.6**
Attitude Rate *(RSS Pitch and Yaw Rate)*	Max	deg/s	2.1	19.3	3.4	2.7	3.6	3.5	17.8	14.1
	Min	deg/s	0.0	0.0	0.0	0.0	0.0	0.0	0.0	0.0
	99%-tile	**deg/s**	**1.7**	**1.8**	**2.1**	**1.7**	**1.8**	**2.0**	**1.7**	**1.9**
Relative Pitch	Max	deg	90.0	90.0	90.0	90.0	90.0	90.0	90.0	90.0
	Min	deg	86.2	65.6	85.4	86.2	85.6	85.7	64.7	52.1
	1%-tile	**deg**	**86.6**	**86.5**	**86.9**	**86.8**	**86.7**	**86.8**	**86.6**	**86.9**

V. Conclusions

The ALHAT POST2-based end-to-end 6DOF simulation provides descent and landing simulation capability to assess various sensor and GNC combinations to optimally design and operate an autonomous system for precision lunar landing. A description of each new or updated ALHAT-specific model currently incorporated into the POST2 end-to-end simulation has been discussed. In addition, a preliminary GNC performance analysis and discussion of the results of the ALHAT precision lunar-landing system Monte Carlos have been presented. Each of the approach phase designs of the ALHAT DAC1 GNC Monte Carlos discussed either met the landing accuracy requirement of a 1-sigma downrange and crossrange variation of less than 30 m for all cases or were within at least 7% of the

requirement. Also, each of the approach phase designs discussed met the preliminary touchdown requirements of 99-percentile vertical velocity less than 2 m/s and 99-percentile horizontal velocity less than 1 m/s. Seven of the eight approach phase designs met the preliminary requirement of 99-percentile attitude rate less than 2 deg/s and all cases met the relative pitch angle preliminary touchdown requirement of the lander greater than 84 deg (1-percentile). Overall, these preliminary Monte Carlo results of the GNC portion of DAC1 show that the ALHAT landing system integrated into the POST2 simulation perform as expected considering the low-fidelity of the sensor models, worst-case sensor configuration and system, vehicle and sensor uncertainties used.

ALHAT DAC1 TSAR and AFM performance analyses are ongoing. Further advancements in ALHAT system-model development will allow the integration of more detailed models such as high-fidelity altimeter, velocimeter, TRN and HRN models. A new and higher-fidelity vehicle model based on the Altair vehicle design will also be implemented into the POST2 simulation in preparation for the ALHAT DAC2, or second stage of the ALHAT landing system performance analysis. The increase in fidelity of the models discussed, and their validation in the POST2 simulation, will expand the capability of the ALHAT POST2-based end-to-end descent and landing trajectory simulation for overall system performance analysis of future lunar-lander systems, especially Altair-type systems.

Acknowledgments

This POST2 simulation work was supported by the Atmospheric Flight and Entry Systems Branch (AFESB) in the System Engineering Directorate at NASA Langley Research Center. Contributors to the ALHAT POST2 simulation include NASA Johnson Space Center, Jet Propulsion Laboratory, Draper Laboratory and University of Texas at Austin. The authors appreciate the support of Chirold Epp, ALHAT project lead, and all members of the ALHAT project team.

References

[1]Epp, C. D., and Smith, T. B., "Autonomous Precision Landing and Hazard Detection Avoidance Technology (ALHAT) Project," IEEE/AC-1379, March 2007.

[2]Bauer, G.L., Cornick, D.E., and Stevenson, R., "Capabilities and Applications of the Program to Optimize Simulated Trajectories (POST)," NASA CR-2770, February 1977.

[3]Fisher, J. L., and Striepe, S. A., "POST2 End-to-End Descent and Landing Simulation for the Autonomous Landing and Hazard Avoidance Technology Project," AAS 07-119, 2007, *AAS Space Flight Mechanics Meeting*, Sedona, AZ, January 2007.

[4]DeMars, K. J. and Bishop, R. H., "Precision Descent Navigation for Landing at the Moon," AAS 07-314, *AAS/AIAA Space Flight Mechanics Meeting*, Mackinac Island, MI, 2007.

[5]DeMars, K. J. and Bishop, R. H., "Navigation Analysis to Facilitate Precision Descent Navigation for Landing at the Moon," AAS 08-168, *AAS/AIAA Space Flight Mechanics Meeting*, Galveston, TX, January 2008.

[6]DeMars, K. J., Bishop, R. H., Crain, T.P., and Condon, G. L., "Engineering Analysis of Guidance and Navigation Performance in the Uncertain Lunar Environment to Support Human Exploration," AAS 08-046, *AAS Guidance and Control Conference*, Breckenridge, CO, February 2008.

[7]Johnson, M.C., "A Parameterized Approach to the Design of Lunar Lander Attitude Controllers," AIAA 2006-6564, August 2006.

[8] Forest, L., Kessler, L., and Homer, M., "Design of a Human- Interactive Autonomous Flight Manager (AFM) for Crewed Lunar Landing," AIAA-2007-2708, September 2007.

[9]Johnson, A., Huertas, A., Werner, R. and Montgomery, J., "Analysis of On-Board Hazard Detection and Avoidance for Safe Lunar Landing," *IEEE Aerospace Conference*, 1095-323X, Big Sky, MO, March 2008, pp. 1-9.

[10]Kelly, T. J., "Manned Lunar Lander Design: The Project Apollo Lunar Module (LM)," AIAA 1992-1480, *AIAA Space Programs and Technologies Conference,* Huntsville, AL., March 1992.